ZnO-based ultraviolet avalanche photodetectors

2013 J. Phys. D: Appl. Phys. 46 305105

(http://iopscience.iop.org/0022-3727/46/30/305105)

J. Phys. D: Appl. Phys. **46** (2013) 305105 (5pp) doi:10.1088/0022-3727/46/30/305105

ZnO-based ultraviolet avalanche photodetectors

J Yu[1,2], C X Shan[1,4], X M Huang[3], X W Zhang[1,2], S P Wang[1] and D Z Shen[1]

[1] State Key Laboratory of Luminescence and Applications, Changchun Institute of Optics, Fine Mechanics and Physics, Chinese Academy of Sciences, Changchun 130033, People's Republic of China
[2] University of Chinese Academy of Sciences, Beijing 100049, People's Republic of China
[3] Jiangsu Provincial Key Laboratory of Advanced Photonic and Electronic Materials, and School of Electronic Science and Engineering, Nanjing University, Nanjing 210093, People's Republic of China

E-mail: shancx@ciomp.ac.cn

Received 2 February 2013, in final form 5 June 2013
Published 2 July 2013
Online at stacks.iop.org/JPhysD/46/305105

Abstract
By virtue of the carrier avalanche multiplication caused by an impact ionization process occurring in MgO insulation layer, zinc oxide (ZnO)-based ultraviolet (UV) avalanche photodetectors (APDs) have been fabricated from Au/MgO/ZnO/MgO/Au structures. The responsivity of APDs can reach 1.7×10^4 A W^{-1}, and the avalanche gain of the photodetectors is about 294 at 73 V. Considering that no previous report on ZnO APDs can be found, the results reported in this paper may promise a route to high-performance ZnO UV photodetectors.

(Some figures may appear in colour only in the online journal)

1. Introduction

Ultraviolet (UV) photodetectors fabricated from wide bandgap semiconductors have a variety of potential applications including missile warning, flame sensing, space communications, etc [1–6]. As a wide bandgap semiconductor, zinc oxide (ZnO) has been regarded as a promising candidate for UV photodetectors for its wide tunable bandgap when alloyed with MgO or BeO [7, 8]. Also, it has been reported that the irradiation-resistance of ZnO is larger than many other wide bandgap semiconductors [9], which makes it suitable for use in harsh environment. Experimentally, various structured ZnO-based photodetectors including metal–semiconductor–metal [10], photoconductive [5], Schottky [11], p–n junction [12], etc, have been demonstrated in recent years. Compared with the above-mentioned structures, avalanche photodetectors (APDs) offer large gain, thus they may have relatively high sensitivity and low noise [13–21]. Nevertheless, since APDs are usually realized in p–n junction based structures, while the reproducible and stable p-type doping of ZnO is still a huge challenge, no report on ZnO APDs can be found up to now.

In this paper, by virtue of carrier multiplication caused by an impact ionization process occurred in MgO insulation layer under relatively large electric field, ZnO APDs have been realized, and the avalanche gain can reach 294 at 73 V bias. We note that although impact ionization occurring in dielectric layer has been employed to increase the responsivity of photodetectors [3, 6, 22], no previous report on ZnO APDs can be found.

2. Experiments

The ZnO films employed as the active layer of the APDs were deposited on sapphire substrates in a magnetron sputtering equipment. Metallic zinc (99.999%) was used as a target for the sputtering, and the sputtering power was fixed at 100 W. A mixed gas of oxygen and argon with a flow ratio of 1 : 1 was employed as the ambient for the sputtering. The working pressure in the growth chamber was maintained at around 1 Pa and the substrate temperature at 300 °C during the sputtering process. A MgO film was deposited onto the as-grown ZnO films in the same magnetic sputtering facility acting as the insulation layer for the impact ionization. Then a thin Au layer was evaporated onto the MgO films using a vacuum evaporation method. Note that the Au electrode was patterned into interdigital configuration via a photolithography and wet etching process. The structural characterization of the films was carried out in a Bruker D8 x-ray diffractometer

[4] Author to whom any correspondence should be addressed.

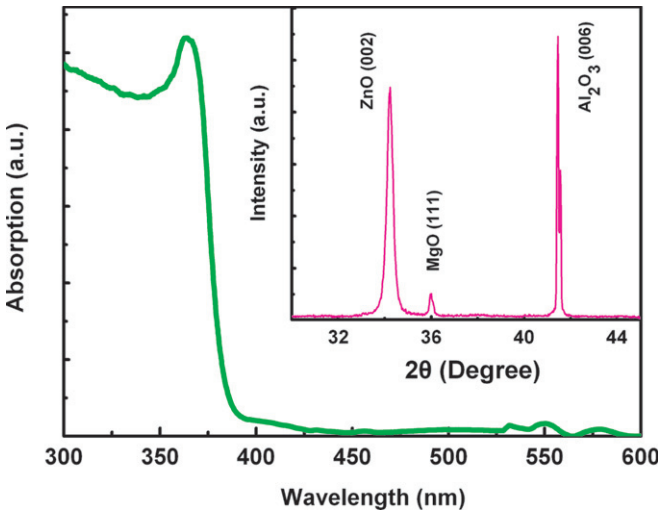

Figure 1. Room temperature absorption spectrum of the ZnO films, and the inset shows the XRD pattern of the MgO coated ZnO films.

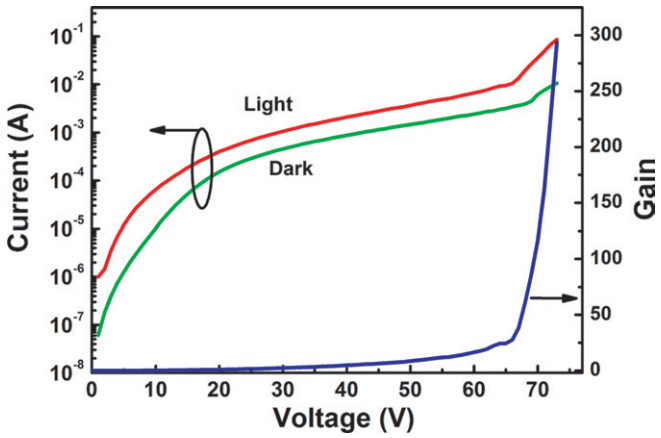

Figure 2. *I–V* characteristics of the ZnO photodetector measured under dark and 380 nm light illumination conditions, and the calculated avalanche gain of the photodetector from equation (2) as a function of the applied bias is also shown in the figure.

employing Cu Kα line ($\lambda = 1.54$ Å) as the excitation source. The absorption spectrum of the ZnO films was studied in a Shimadzu UV-3101 PC scanning spectrophotometer. The electrical characteristics of the films and the photodetectors were measured in a Lakeshore 7707 Hall measurement system. The photoresponse of the photodetectors was measured in a SPEX scanning monochromator employing a 150 W Xe lamp as the illumination source. The temporal response of the ZnO APDs was measured under the excitation of the 266 nm line of a Nd : YAG laser with the pulse width of 10 ns, and the transient signals were recorded by a Triax 550 spectrograph.

3. Results and discussion

Hall measurement reveals that the ZnO film shows n-type conduction with an electron concentration of 9.2×10^{16} cm^{-3} and a Hall mobility of 2.0 cm^2 V^{-1} s^{-1}. Figure 1 shows the absorption spectrum of the ZnO film. It can be seen that the film has a strong absorption in the UV spectrum region, while it is almost transparent in the visible region. The above characters are favourable for its application in high-performance UV photodetectors. There appears an absorption edge at around 383 nm, which corresponds to the near-band-edge absorption of ZnO. The inset of figure 1 illustrates the x-ray diffraction (XRD) pattern of the MgO coated ZnO films. Besides the diffraction from the sapphire substrate, two other diffraction peaks can be observed. The peak located at 34.2° can be indexed to the diffraction from (0 0 2) facet of wurtzite ZnO, while the other peak at 36.0° comes from the diffraction of the (1 1 1) facet of cubic rocksalt MgO.

The current–voltage (I–V) characteristics of the Au/MgO/ZnO/MgO/Au structure measured under dark and 380 nm light illumination conditions are shown in figure 2. Note that the dark current of the device is about 61 nA at 1 V bias, while it increases to around 10 mA when the bias reaches 73 V, and the relatively large dark current may come from the structural imperfections in the ZnO films. Both the photocurrent and dark current increase rapidly with the applied bias initially, then saturate gradually when the applied voltage is larger than 20 V, and the current increases rapidly again when the bias voltage is over 68 V, indicating that a carrier avalanche multiplication may occur then. The avalanche gain (M) of the structure can be determined using the following expression [23]:

$$M = \frac{I_{\mathrm{ph}} - I_{\mathrm{d}}}{I_{\mathrm{ph0}} - I_{\mathrm{d0}}}, \tag{1}$$

where I_{ph} and I_{d} are the multiplied photocurrent and dark current, while I_{ph0} and I_{d0} are the unmultiplied photocurrent and dark current, respectively. According to the photocurrent curve of the structure shown in figure 2, the photocurrent increases rapidly with bias initially, then tends to saturate when the bias voltage is over 20 V. Therefore, the current at 20 V has been regarded as the unmultiplied current, which is about 3.4×10^{-4} A for unmultiplied photocurrent and 1.5×10^{-4} A for unmultiplied dark current. The calculated avalanche gain from equation (1) at various bias voltages is also shown in figure 2. One can see from the figure that the avalanche gain increases gradually with the bias voltage, and it rises abruptly when the bias is larger than 68 V. The abrupt increase of the avalanche gain at larger bias suggests that carrier avalanche multiplication has occurred. The gain reaches 294 when the bias voltage is 73 V (limited by the test facility current compliance set at 100 mA). Note that the avalanche gain in our case is comparable to the corresponding values reported in GaN-based APDs, for example, Tut *et al* reported an avalanche gain of 25 at 72 V [24]. McClintock *et al* showed an avalanche gain of 700 at 60 V [25]. Zheng *et al* reported an avalanche gain of 30–400 in GaN p-i-p-i-n structured APD [26]. Xie *et al* demonstrated an avalanche gain of 1100 at 140 V [16] and Bayram *et al* reported an avalanche gain of 51000 at 85 V [18].

The response spectrum of the Au/MgO/ZnO/MgO/Au structure at 73 V is shown in figure 3. The spectrum shows a maximum responsivity of 1.7×10^4 A W^{-1} at around 367 nm. We note that the position for the maximum responsivity depends both on the absorption coefficient and quantum efficiency of ZnO, thus it may deviate from the corresponding wavelength of the ZnO bandgap (around 375 nm) [27, 28].

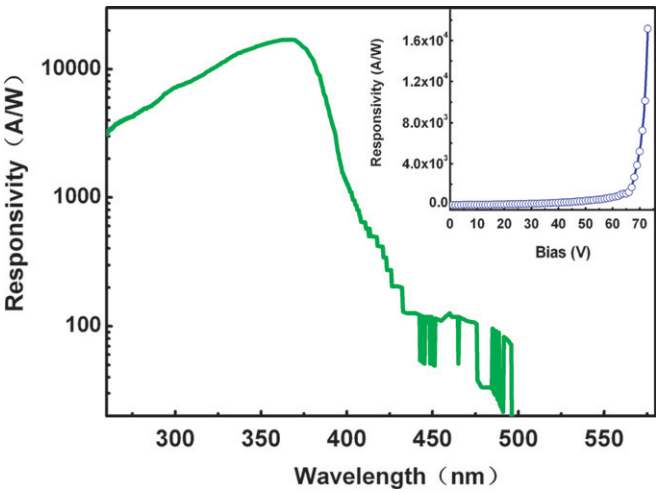

Figure 3. A typical photoresponse spectrum of the photodetector biased at 73 V, and the inset shows the responsivity of the photodetector as a function of the applied bias.

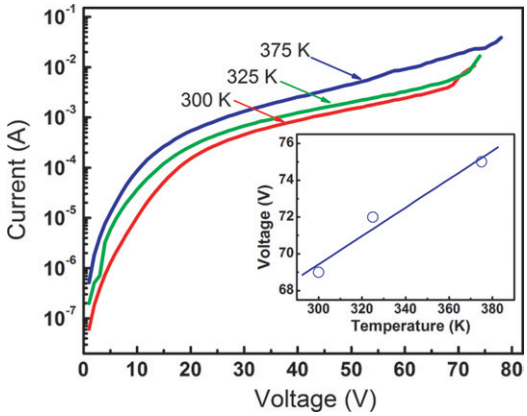

Figure 4. *I–V* characteristics of the photodetector recorded at 300, 325 and 375 K under dark conditions, and the inset shows the dependence of the avalanche breakdown voltage on recording temperature.

Another noteworthy phenomenon in the response spectrum lies in the relatively high responsivity, indicating high optical gain has occurred in the structure. The inset of figure 3 shows the maximum responsivity of the photodetector as a function of the applied bias. One can see from the figure that the maximum responsivity increases gradually when the bias voltage is small, but it increases abruptly when the bias is over 65 V. The above phenomenon consolidates the fact that carrier avalanche multiplication has occurred in the Au/MgO/ZnO/MgO/Au structure. The detectivity (D^*) of a photodetector can be determined by the following expression [29]:

$$D^* = \frac{R}{\sqrt{2qJ_d}}, \tag{2}$$

where R is the responsivity of the photodetector, q is the elemental charge and J_d is the dark current density. Considering that $R = 1.7 \times 10^4\,\mathrm{A\,W^{-1}}$, $J_d = 8.8\,\mathrm{A\,cm^{-2}}$, one can deduce that the detectivity of the photodetector $D^* = 3.2 \times 10^{12}$ Jones from equation (2).

There are three possible mechanisms that may be responsible for the high optical gain in a photodetector, that is photoconductive gain, Zener tunnelling and avalanche multiplication. It has been reported that Zener tunnelling usually occurs in highly doped semiconductors under small bias, while in our case, the ZnO films have not been doped at all, so the optical gain caused by Zener tunnelling may not exist in the Au/MgO/ZnO/MgO/Au structure. Another proof for excluding Zener tunnelling is that the optical gain caused by Zener tunnelling usually has a negative temperature coefficient [23], while a positive temperature coefficient has been observed in the Au/MgO/ZnO/MgO/Au structured photodetector, as indicated in figure 4. In this figure, the carrier avalanche multiplication characteristics of the photodetector have been measured as a function of temperature. One can see that the critical avalanche voltage increases obviously with temperature, demonstrating a positive thermal coefficient of $0.08\,\mathrm{V\,K^{-1}}$. The above results rule out the possibility that Zener tunnelling dominates the gain. As for the photoconductive gain, it usually increases linearly with bias voltage firstly, and then saturates gradually when the bias is increased further [16, 30]. Instead, in figure 2, one can see that the gain of the photodetector increases gradually then abruptly with applied voltage, which is contrary to the bias dependence of photoconductive gain, thus the photoconductive gain cannot be the dominant factor in our case although it may contribute to the response of the photodetector. Based on the above data, the optical gain in the Au/MgO/ZnO/MgO/Au structured photodetector should be dominated by the carrier avalanche multiplication.

The mechanism for the avalanche gain in the ZnO APDs can be understood as follows: when light is illuminated onto the Au/MgO/ZnO/MgO/Au structure, electrons and holes will be generated in the ZnO layer. When the bias voltage is applied onto the structure, some of the residual carriers and photogenerated carriers will be drifted into the MgO layer driven by the voltage. Considering that the Au/MgO/ZnO/MgO/Au structure is composed of two Schottky barriers connected back-to-back, bias of any polarity will put one Schottky barrier reverse-biased and the other forward-biased [31]. With the increase of the bias, the barrier height in the forward direction is lowered and that in the reverse direction is enhanced. Most of the voltage will be applied onto the MgO layer lied in the reverse bias contact considering the dielectric nature of the MgO layer. Then carriers that enter into the MgO layer from the ZnO layer will be accelerated greatly under such a strong electric field. The accelerated carriers may impact with the lattice of the MgO layer to release their kinetic energy and generate additional electrons and holes. The generated electrons and holes will again gain much kinetic energy from the electric field and generate more other electrons and holes. In this way, carrier avalanche multiplication occurs and the current increases rapidly [32–34]. The generated electrons and holes will be separated by the bias voltage and collected by the corresponding electrodes. As a result, great optical gain has been achieved. Note that APD may also be realized in single Schottky structure, but in the Au/MgO/ZnO/MgO/Au structures, the APD can work under bias with any polarity,

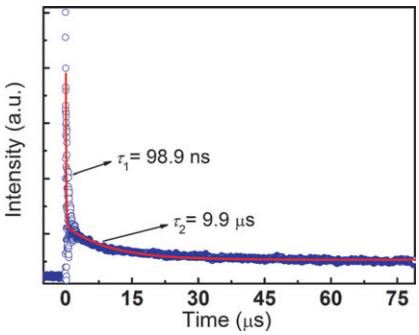

Figure 5. Photoresponse decay of the photodetector, in which the scattered circles are experimental data, while the solid line is the fitting results to the experimental data using a two-order exponential decay formula.

which is one of the major advantages of these structures compared with their single Schottky structured counterparts.

The response time of the Au/MgO/ZnO/MgO/Au structured APDs has been measured, and the results of which are shown in figure 5. One can see from the experimental data shown by scattered circles that the response rise time of the APD is around 20 ns, while the decay time can be well fitted using a two-order exponential formula shown below [30]:

$$I = A_1 \exp(-t/\tau_1) + A_2 \exp(-t/\tau_2) + I_0 \qquad (3)$$

where I and I_0 is the response intensity of the photodetector, t is time, τ_1 and τ_2 are decay lifetimes, A_1 and A_2 are constant. The best fitting yields $\tau_1 = 98.9$ ns and $\tau_2 = 9.9\,\mu$s. The above results confirm that there are two gain channels in the photodetector, and the lifetime of the fast one is about 98.9 ns, while that of the slow one is about 9.9 μs. The fast one may come from the avalanche gain, and the slow one from the photoconductive gain. As for the origin of the photoconductive gain, it may come from the carrier trapping by the structural imperfections at the MgO/ZnO interface [35]. The temporal response results confirm that photoconductive gain also contributes to the photoresponse of the structure, although avalanche multiplication dominates the gain of the APD.

To show the electric field distribution and where the carrier multiplication prefers to happen, the electric field distribution of the Au/MgO/ZnO/MgO/Au structure is simulated using COMSOL Multiphysics software. The inset of figure 6 shows the schematic illustration of the ZnO APD and the electric field distribution in the structure. The thickness of the ZnO film is about 300 nm, and that of the MgO layer is about 60 nm. The thickness of the Au film is about 100 nm, the length of the Au interdigital electrode is 500 μm, the width of the Au interdigital electrode is 5 μm, the inter-electrode spacing is 5 μm. Considering that the electron effective mass of ZnO is 0.29 m_0, and the permittivity of the ZnO and MgO are 8.66 and 9.65, respectively, the surface electric field profile of the structure biased at 68 V under dark conditions is illustrated in figure 6. One can see that most of the electric field is loaded along the edge of the reverse-biased finger electrode, which means that impact ionization will initiate there, and the critical electrical field in this region is about 15.7 MV cm^{-1}.

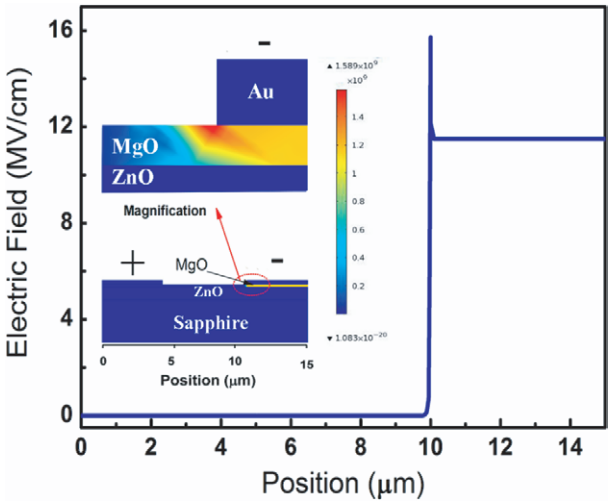

Figure 6. Simulated surface electric field profile of the Au/MgO/ZnO/MgO/Au structure at 68 V, and the inset shows a schematic diagram of the structure and the electric field distribution in the structure.

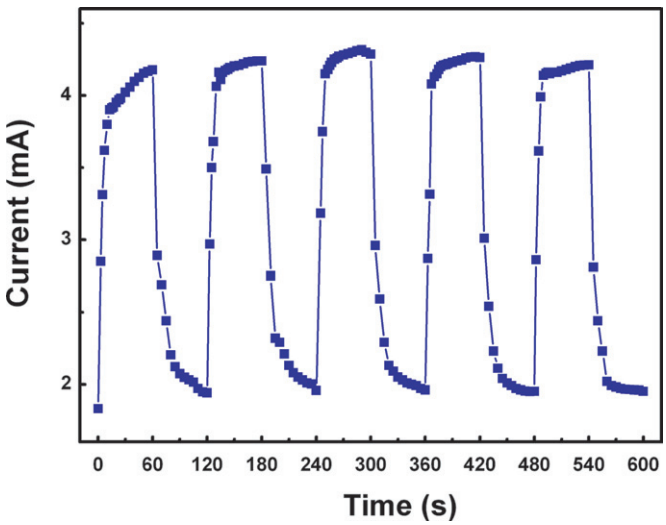

Figure 7. Time-resolved photocurrent of the ZnO APD with UV light on and off for five cycles at a bias voltage of 68 V.

Stability is an important parameter for an APD. To evaluate the stability of the ZnO APD, time-resolved photocurrent of the device has been measured with the illumination of 367 nm UV light on and off repeatedly for five cycles at 68 V, and the results of which are shown in figure 7. One can see from the figure that the device shows little degradation in the investigated time scale, indicating the good stability of the APDs.

4. Conclusions

In summary, ZnO APDs have been demonstrated from Au/MgO/ZnO/MgO/Au structures, and the APD exhibits a responsivity of 1.7×10^4 A W^{-1} and an avalanche gain of 294 at 73 V bias. The gain comes mainly from the carrier avalanche multiplication realized in the MgO layer via an impact ionization process under relatively large electric field.

The results reported in this paper may promise a route to high-performance ZnO UV photodetectors.

Acknowledgments

This work is supported by the National Basic Research Program of China (2011CB302006), the Natural Science Foundation of China (11134009, 11104265 and 61177040) and the Science and Technology Developing Project of Jilin Province (20111801).

References

[1] Razeghi M and Rogalski A 1996 *J. Appl. Phys.* **79** 7433
[2] Ali G M and Chakrabarti P 2010 *J. Phys. D: Appl. Phys.* **43** 415103
[3] Wang W J, Shan C X, Zhu H, Ma F Y, Shen D Z, Fan X W and Choy K L 2010 *J. Phys. D: Appl. Phys.* **43** 045102
[4] Xing J, Wei H Y, Guo E J and Yang F 2011 *J. Phys. D: Appl. Phys.* **44** 375104
[5] Liu J S, Shan C X, Li B H, Zhang Z Z, Yang C L, Shen D Z and Fan X W 2010 *Appl. Phys. Lett.* **97** 251102
[6] Zhu H, Shan C X, Wang L K, Zheng J, Zhang J Y, Yao B and Shen D Z 2010 *J. Phys. Chem. C* **114** 7169
[7] Tabares G, Hierro A, Ulloa J M, Guzman A, Munoz E, Nakamura A, Hayashi T and Temmyo J 2010 *Appl. Phys. Lett.* **96** 101112
[8] Ryu Y R, Lee T S, Lubguban J A, Corman A B, White H W, Lee J H, Han M S, Park Y S, Youn C J and Kim W J 2006 *Appl. Phys. Lett.* **88** 052103
[9] Look D C, Reynolds D C, Hemsky J W, Jones R L and Sizelove J R 1999 *Appl. Phys. Lett.* **75** 811
[10] Ju Z G, Shan C X, Jiang D Y, Zhang J Y, Yao B, Zhao D X, Shen D Z and Fan X W 2008 *Appl. Phys. Lett.* **93** 173505
[11] Endo H, Sugibuchi M, Takahashi K, Goto S, Sugimura S, Hane K and Kashiwaba Y 2007 *Appl. Phys. Lett.* **90** 121906
[12] Liu K W, Shen D Z, Shan C X, Zhang J Y, Yao B, Zhao D X, Lu Y M and Fan X W 2007 *Appl. Phys. Lett.* **91** 201106
[13] McClintock R, Pau J L, Minder K, Bayram C, Kung P and Razeghi M 2007 *Appl. Phys. Lett.* **90** 141112
[14] Bai X G, Liu H D, McIntosh D C and Campbell J C 2009 *IEEE J. Quantum Electron.* **45** 300
[15] Pau J L, McClintock R, Razeghi M and Silversmith D 2008 *Appl. Phys. Lett.* **92** 101120
[16] Xie F, Lu H, Chen D J, Xiu X Q, Zhao H, Zhang R and Zheng Y D 2011 *IEEE Electron Device Lett.* **32** 1260
[17] Carrano J C, Lambert D J H, Eiting C J, Collins C J, Li T, Wang S, Yang B, Beck A L, Dupuis R D and Campbell J C 2000 *Appl. Phys. Lett.* **76** 924
[18] Bayram C, Pau J L, McClintock R and Razeghi M 2008 *Appl. Phys. Lett.* **92** 241103
[19] Minder K, Pau J L, McClintock R, Kung P, Bayram C and Razeghi M 2007 *Appl. Phys. Lett.* **91** 073513
[20] Bayram C, Pau J L, McClintock R, Razeghi M, Ulmer M P and Silversmith D 2008 *Appl. Phys. Lett.* **93** 211107
[21] Yu J, Shan C X, Liu J S, Zhang X W, Li B H and Shen D Z 2013 *Phys. Status Solidi Rapid Res. Lett.* **7** 425
[22] Yu J, Shan C X, Qiao Q, Xie X H, Zhang Z Z, Wang S P and Shen D Z 2012 *Sensors* **12** 1280
[23] Sze S M and Ng K K 2007 *Physics of Semiconductor Devices* 3rd edn (Hoboken, NJ: Wiley)
[24] Tut T, Butun S, Butun B, Gokkavas M, Yu H and Ozbay E, 2005 *Appl. Phys. Lett.* **87** 223502
[25] McClintock R, Yasan A, Minder K, Kung P and Razeghi M, 2005 *Appl. Phys. Lett.* **87** 241123
[26] Zheng J Y, Wang L, Hao Z B, Luo Y, Wang L X and Chen X K 2012 *Chin. Phys. Lett.* **29** 097804
[27] Liu C Y, Zhang B P, Lu Z W, Binh N T, Wakatsuki K, Segawa Y and Mu R 2009 *J. Mater. Sci. Mater. Electron.* **20** 197
[28] Bi Z, Zhang J W, Bian X M, Wang D, Zhang X N, Zhang W F and Hou X 2008 *J. Electron. Mater.* **37** 760
[29] Gong X, Tong M, Xia Y, Cai W, Moon J S, Cao Y, Yu G, Shieh C L, Nilsson B and Heeger A J 2009 *Science* **325** 1665
[30] Moustakkas T D and Misra M 2007 *Proc. SPIE* **6766** 67660C
[31] Sze S M, Coleman D J and Loya A 1971 *Solid-State Electron.* **14** 1209
[32] Zhu H *et al* 2010 *Adv. Mater.* **22** 1877
[33] Ma X Y, Chen P L, Li D S, Zhang Y Y and Yang D R 2007 *Appl. Phys. Lett.* **91** 251109
[34] Zhu H, Shan C X, Li B H, Zhang Z Z, Shen D Z and Choy K L 2011 *J. Mater. Chem.* **21** 2848
[35] Farmer J W and Lee R S 1975 *J. Appl. Phys.* **46** 2710